

Analysis of Texture-Induced Anisotropy in Drawn Molybdenum Rods

Student Names: Saurav Basu, Grant Carnal, Harley Clark, Katie Mullins, Allison Thornton

Faculty Advisors: Professor John Blendell

Industrial Sponsors: Wei-Hsun Chen, Yuanyuan Jing

Improving ASML's lithography machine requires the anisotropic behavior of molybdenum to be integrated into their finite element analysis (FEA) to more accurately model the pressure capacity of the droplet generator. Using a two-pronged approach, in which mechanical testing and mathematical approximations determine the moduli of the molybdenum rod. The mechanical testing includes tensile, torsion, and ultrasonic tests. The mathematical approximation defines the stiffness matrix based on a sufficient number of moduli sampled in different orientations with regard to the sample geometry. Electron backscatter diffraction imaging and x-ray diffraction are used to evaluate the texture of the rod and inform our assumptions when performing the aforementioned approach. Comparing this determined texture to a reference orientation distribution function allows for better refinement of the mathematical approximations. Accounting for these orientations in the sample orientations throughout mechanical testing maintains consistency and provides an accurate determination of the stiffness matrix.

This work is sponsored by ASML, San Diego, CA



Background

Molybdenum (Mo) is a BCC refractory and trace metal which features a high melting point and a low coefficient of thermal expansion, making Mo the metal of choice for high-temperature applications. The forged and drawn molybdenum rods used by ASML indicate applied cold work. The deformation of grains induced during processing leads to anisotropic mechanical properties. Cold work creates uneven plastic deformation of grains. These grains have certain orientations after deformation, depending on the method by which they were worked. If the grains of a material are similarly oriented, then the natural anisotropy of each grain is not canceled out by the bulk of the material, and a "texture" of mechanical properties is formed.

ASML requires a model that can accurately integrate anisotropic textures into their FEA, which does not currently account for the anisotropy of the material's texture from the specific processing history of the rods. In ignoring anisotropy present within the drawn rods there is an over or underestimation for their strength.

Experimental Procedure

Texture Analysis EBSD

A Quanta 650 was used to scan the face of the Mo in the axial direction to determine the presence of texture. Each scan was run at 20 kV with a spot size of 5.0. These results were analyzed and used to generate an orientation distribution function to mathematically predict the mechanical properties of the rod.

XRD

A Bruker D8 Focus was used to scan the Mo in the XY and YZ directions to determine the presence of texture. The scan intensities were normalized and compared to the JCPDS standard scan of Mo. MRD values were calculated for each direction, a larger value correlated to texture in a preferred orientation.

Mechanical Testing

Tensile Testing

A MTS tensile test frame was used to determine the tensile behavior of the material in the radial direction. The machine has a 100 kN load cell and the test is run at a strain rate of 0.036 mm/min.

Torsion Testing

A MTS torsion testing rig was used to determine the shear behavior of the material. Cylindrical rods were cut and machined in the axial direction to meet specifications before testing to a full 35° rotation angle over 700 seconds.

Ultrasonic

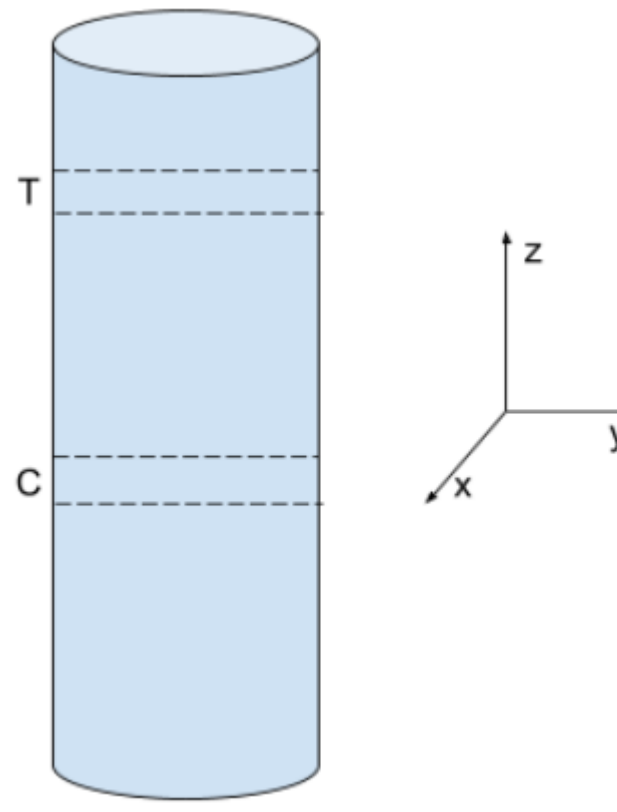
An ultrasonic pulse generator and oscilloscope were used to determine shear components of C_{11} , C_{12} , and C_{44} of two rectangular prisms (top and center) cut from a cylindrical Mo rod. Respective thicknesses for each side and the density of pure Mo were collected from both samples. Shear and longitudinal transducers were placed on the flat samples with a coupling agent of honey to develop pulses, which were then downloaded to be modelled. An average time difference between pulses and a 15 us time frame were factored with the respective thickness along with the density of Mo in a series of formulas to calculate the velocity, Poisson's ratio, and the previously mentioned shear components. All experimental data is compared to isotropic and anisotropic literature values for validity.

Mathematical Model of Stiffness

Techniques such as the one outlined by Bölke and Bertram can be used to estimate the stiffness matrix based on an ODF generated by diffraction methods such as EBSD. By rotating the literature tensor for the stiffness of a single-crystal sample of the material based on the ODF, the stiffness tensor can be aggregated via an arithmetic mean to simulate the effective stiffness of the distribution of grains in the material. It is important to note that this method assumes all grains in the material are similar, and does not include any information regarding the effects of grain boundaries.

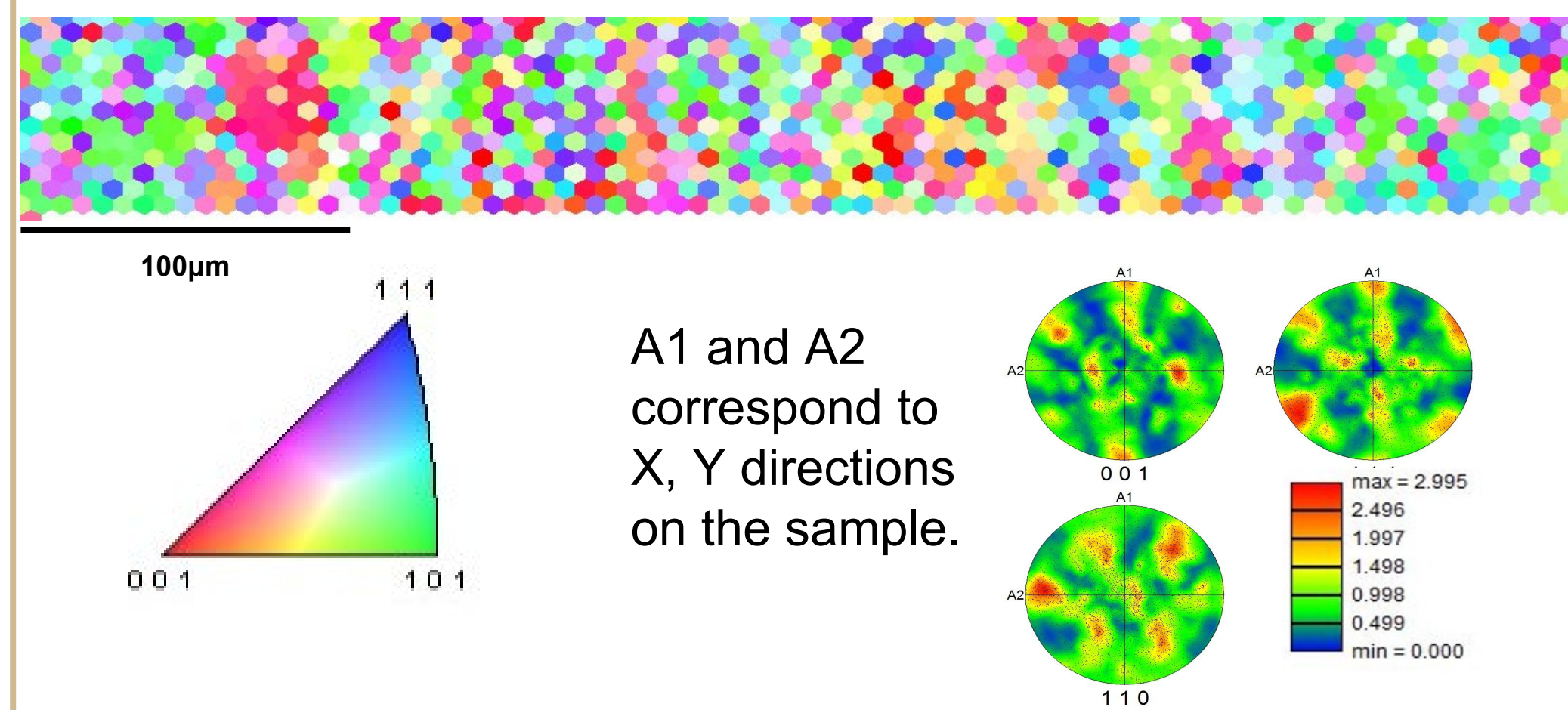
Results & Discussion

As shown to the right, the samples from the Mo rod are sectioned discs cut in the areas mark T and C. With Z being in the axial direction and X and Y orthogonal to one another in the radial directions.



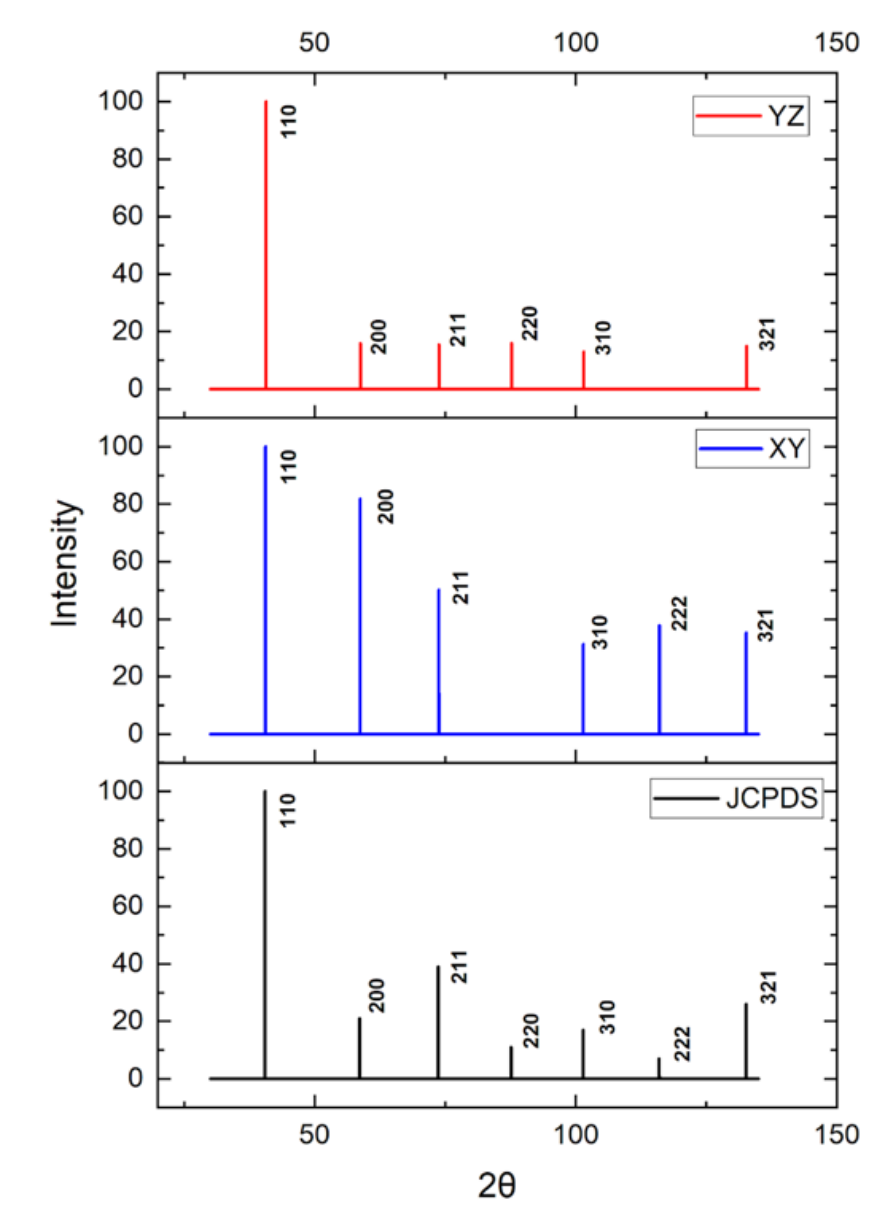
Texture Analysis: EBSD

The inverse pole figure mapping and pole figure projections in the axial direction show that there is likely a weak texture throughout the sample.



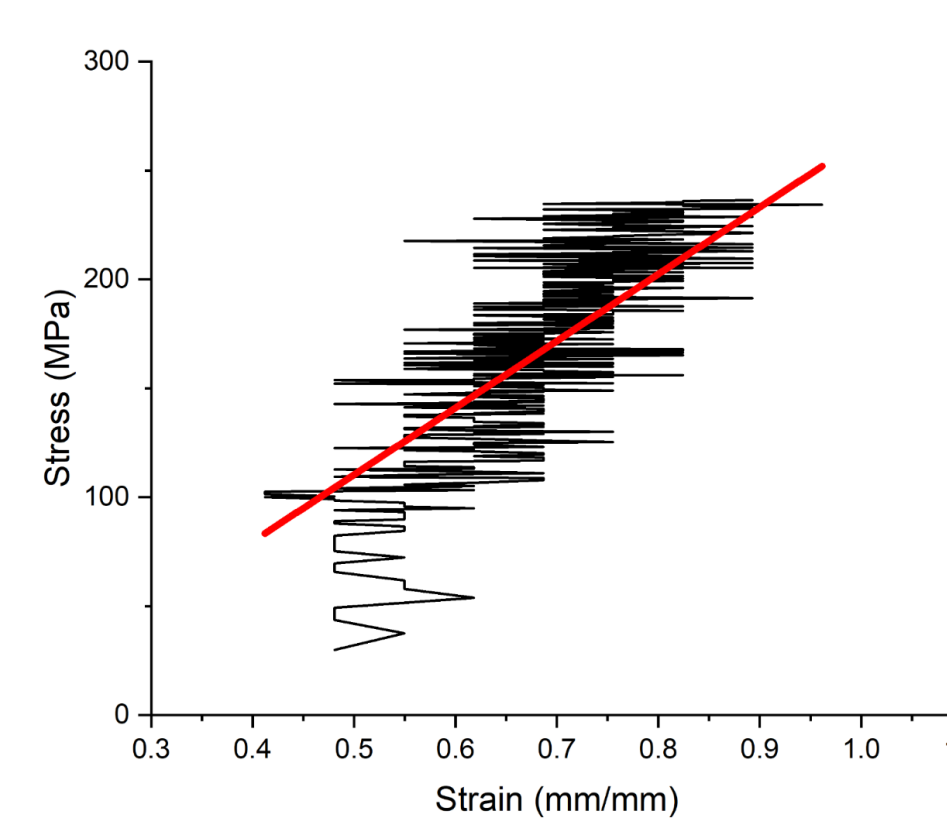
Texture Analysis: XRD

The figure shown depicts the diffraction patterns of the YZ, XY, and JCPDS card.¹ The largest MRD values calculated from these YZ and XY scans were 1.83 in the 220 and 3.55 in the 222 respectively. The larger the MRD value, the greater the texture present. These values do not correspond to perpendicular directions within the crystal lattice it is likely that the Mo rod is not significantly textured, but some texture may be present.



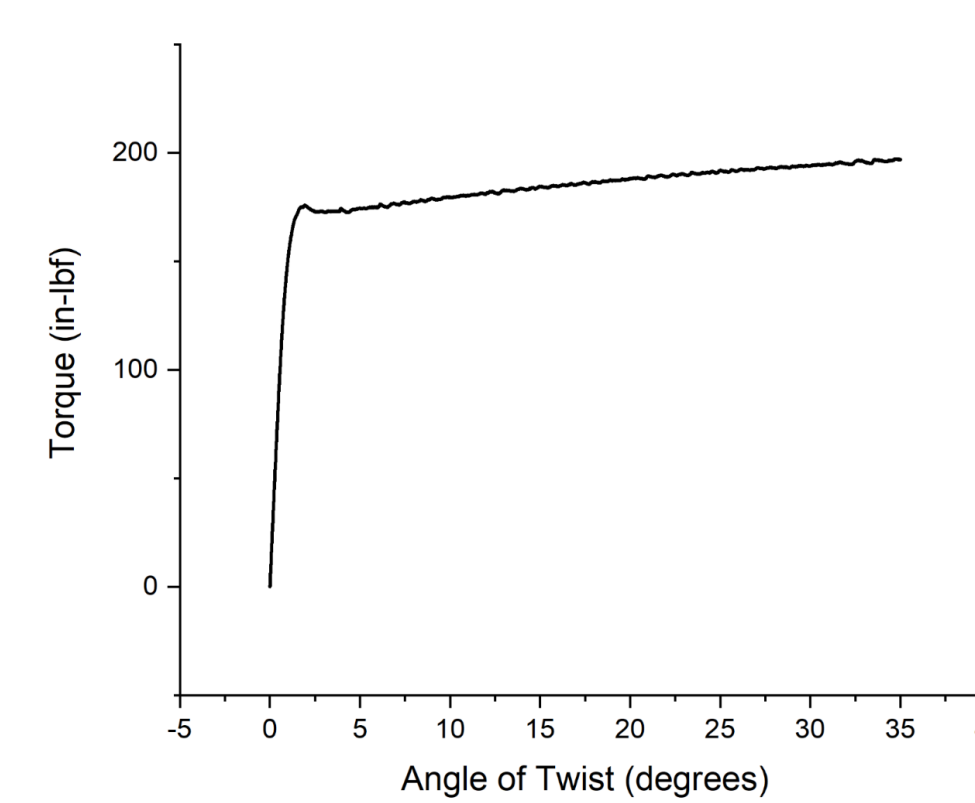
Mechanical Testing: Tensile Testing

Using the determined stress strain curve for the samples the slope of the elastic region can be used to determine the elastic modulus corresponding to the radial stiffness value. This is calculated to be about 307.18 MPa. Due to the irregularities seen in the tensile test, this value is likely to be inaccurate.



Mechanical Testing: Torsion Testing

Torque vs angle of twist from the torsion testing was converted to stress vs strain. The elastic modulus was calculated to be 4.26 GPa. This too does not agree with literature, indicating a larger-scope issue with our mechanical test methodology.



Mechanical Testing: Ultrasonic Testing

T LONG	dt (us)	Thickness (mm)	Velocity (m/s)	Poissons
"Small" (X)	4.64	15.25	6573.28	1.767
"Medium" (Y)	3.78	11.91	6301.59	1.347
"Large" (Z)	3.08	9.84	6389.61	1.561
C LONG				
"Small" (X)	4.71	14.82	6292.99	1.374
"Medium" (Y)	3.76	12.00	6382.98	1.192
"Large" (Z)	3.03	9.86	6508.25	1.393

T SHEAR	dt (us)	Thickness (mm)	Velocity (m/s)	Poisson
"Small" (X)	3.61	15.25	8448.75	1.767
"Medium" (Y)	2.42	11.91	9842.98	1.347
"Large" (Z)	2.24	9.84	8785.71	1.561
C SHEAR				
"Small" (X)	3.08	14.82	9623.38	1.374
"Medium" (Y)	1.98	12.00	12121.21	1.192
"Large" (Z)	2.01	9.86	9810.95	1.393

The tables provide a summary of the calculations collected

T	C11 (GPa)	C44 (GPa)
"Small" (X)	441.59	729.52
"Medium" (Y)	405.84	990.16
"Large" (Z)	417.25	788.87
C		
"Small" (X)	404.73	946.47
"Medium" (Y)	416.39	1501.56
"Large" (Z)	432.89	983.72

to calculate the shear components of C_{11} and C_{44} .

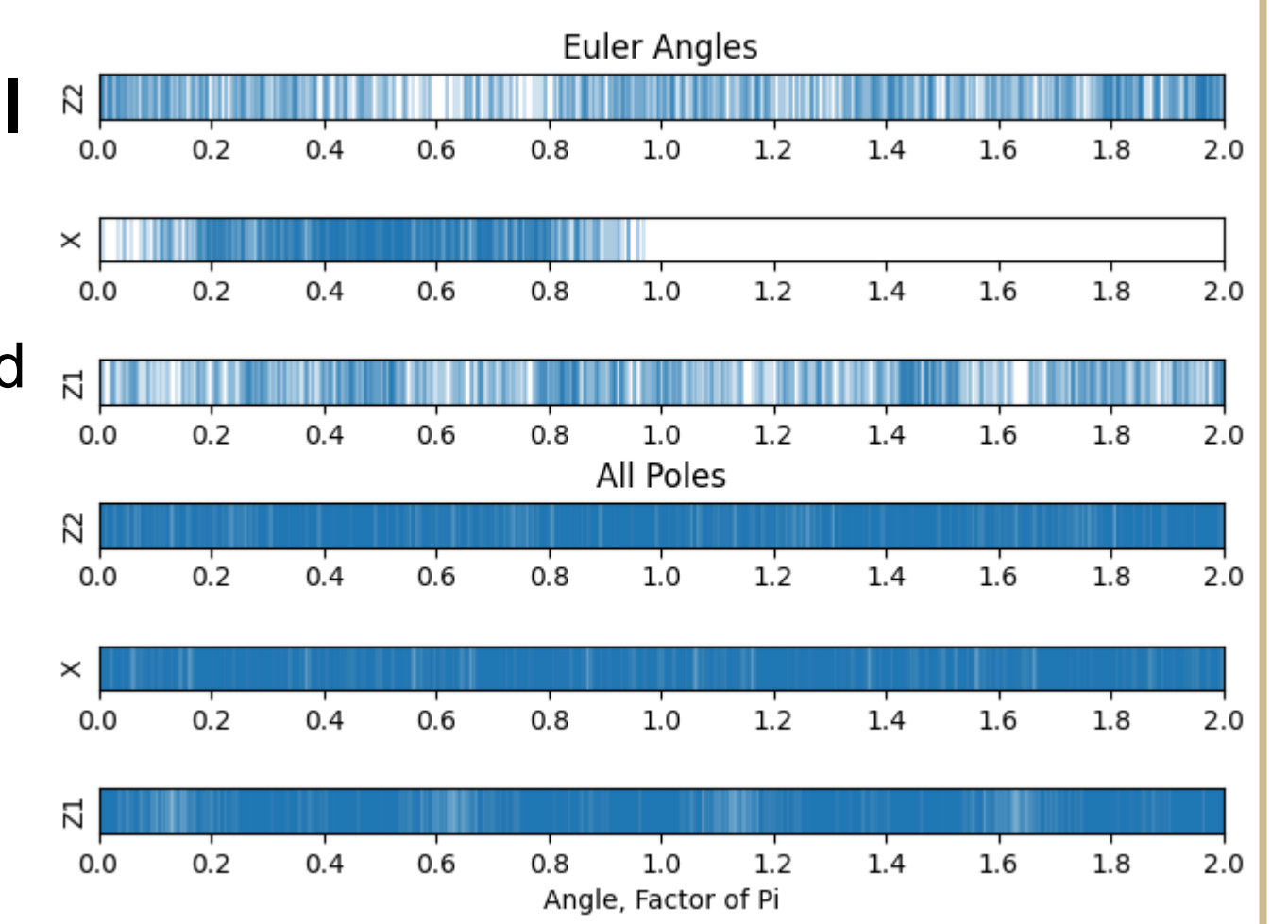
Results & Discussion

	C_{11}	C_{12}	C_{44}	Literature reference values for ultrasonic testing. ²
Isotropic	394 GPa	167 GPa	113 GPa	
Single Crystal Anisotropic	470 GPa	168 GPa	107 GPa	

The C_{11} values were near the reference literature, the C_{44} was far off the reference literature, and C_{12} was not able to be calculated due to sample machining obstacles creating an unworkable $C_{11}^{45^\circ}$. Imperfect sample geometry and data collection issues seem to have caused these disagreements.

Mathematical Model of Stiffness

Euler space quantized from EBSD "Scan A", and the resultant Voigt stiffness matrix from rotated single crystal values² in GPa. Small ($<10^{-1}$) numbers have been culled for clarity.



$$C_{calculated} = \begin{bmatrix} 406.943 & 181.513 & 197.174 & 0 & 0 & 0 \\ 181.513 & 397.155 & 206.962 & 0 & 0 & 0 \\ 197.174 & 206.962 & 381.494 & 0 & 2.306 & 0 \\ 0 & 0 & 0 & 157.182 & 0 & 0 \\ 0 & 0 & 2.306 & 0 & 147.394 & 0 \\ 0 & 0 & 0 & 0 & 0 & 131.733 \end{bmatrix} GPa$$

The stiffness matrices found using mechanical, ultrasonic and mathematical methods vary significantly in the range of 1-100 GPa. Literature values for isotropic Mo yield stiffness matrices where $C_{11} \sim 430$, $C_{12} \sim 180$, $C_{44} \sim 130$ (GPa), lower than our results for ultrasonic, and orders of magnitude higher than our mechanical testing results. The stiffnesses generated by the mathematical model are similar to the expected values, but the 11, 22, and 33 axes vary slightly due to the anisotropy of the sample. Our results are as follows:

	C_{11} (GPa)	C_{12} (GPa)	C_{44} (GPa)
Mechanical	5.7150	-2.8050	4.26
Ultrasonic	419.78 ± 14.74	—	898.3 ± 457.74
Calculated	395.20 ± 12.84	195.22 ± 12.84	145.44 ± 12.84

Agglomerating these values assume a cubic symmetry which is likely inaccurate, requiring quantization of the axes individually. The mechanical values do not appear to reflect reasonable reality.

Recommendations & Conclusion

We found a large range of values through different methods. The lack of agreement means our results are inconclusive. Going forward, we recommend:

- Refine polishing procedure for samples to clarify EBSD.
- Perform failure analysis to diagnose unexpected mechanical behavior.
- Repeat benchmarking and diagnose potential equipment calibration and operation issues.
- Repeat analysis with improved methodologies to find agreeing results.

References

- [1] JCPDS Card Number Mo-00-004-0809.
[2] Simmons, G., & Wang, H. (1971). *Single Crystal Elastic Constants and calculated aggregate properties*. M.I.T. Pr.

Acknowledgements

We would like to thank our sponsors from ASML, Wei-Hsun Chen and Yuanyuan Jing for the assistance throughout the project. We would also like to thank those at Purdue that aided in the progress of this project: Professor Blendell for guiding the team and project, Tom Mann, Anyu Shang, Steven Lorenz, and Talukder Alam for their assistance in specimen preparation and testing.